Research Article

Study of Temperature and Wear Variations of Aluminium in General Dry Sliding Contact

Jawad Ali Shakoor Malik* and Saiprasit Koetniyom
The Sirindhorn International Thai German Graduate School of Engineering, King Mongkut's University of Engineering and Technology North Bangkok, Bangkok, Thailand

Abdelkrim Lamjahdy and Bernd Markert
Institute of General Mechanics (IAM), RWTH Aachen University, Germany

* Corresponding author. E-mail: jawad.a-ae2014@tggs-bangkok.org DOI: 10.14416/j.ijast.2017.12.006
Received: 29 January 2017; Accepted: 15 August 2017; Published online: 15 December 2017

Abstract
The present research focuses on the study of temperature and wear variations of aluminium in general dry sliding contact conditions. The main aim of this research is to develop a simulation methodology in order to calculate temperature and wear variations of different materials (here: aluminium on cast iron) in general dry sliding contacts. The developed simulation methodology is based on an uncoupled thermo-mechanical and wear analysis. The widely spread finite element software Abaqus is used for the numerical investigations. For calibration and validation, experimental investigations are performed with a pin-on-disc test bench. A comparison between the experimental and the numerical results is presented and discussed. The experimental results are in close agreement with the numerical results. For the considered test case (rotational velocity of the disc=300 rpm and load on the pin=110 N) the numerical analysis predicts a maximum temperature of 63°C in comparison to 65°C in the experiment. For the considered test case (rotational velocity of the disc=600 rpm and load on the pin=150 N) the simulation predicts a maximum temperature of 93°C in comparison to 97°C in the experiment. The study concludes that the developed simulation methodology is accurate and can be used to calculate temperature and wear variations of different materials in general dry sliding contact.

Keywords: Frictional heat generation, Pin-on-disc test bench, Thermo-mechanical analysis

1 Introduction

The automotive industry today has gone through many technological advancements. Each year a new car model comes that ensures better performance than the previous model. These cars have the tendency to accelerate and decelerate fast. Brakes are one of the main critical components of the automobiles, because they are used in order to stop or decelerate the vehicle. Brakes are usually categorized as service brakes and parking brakes. Service brakes are used in order to stop the vehicle, while parking brakes allow the vehicle to remain stationary when parked. Service brakes are of many types depending upon their construction, materials and functions, i.e. drum brakes, disc brakes, electric brakes, hydraulic brakes and air brakes. A disc brake is most widely used in automobiles and high speed railways. Automobile disc brake systems comprise of brake caliper, brake pad, caliper holder and brake disc. The driver applies the braking force by pressing the brake pedal, which is converted into hydraulic pressure in the brake caliper. The hydraulic pressure is exerted on the brake pad and as a result the brake pad comes in contact with the brake disc. The rotational energy of

Please cite this article as: J. A. S. Malik, S. Koetniyom, A. Lamjahdy, and B. Markert, "Study of temperature and wear variations of aluminium in general dry sliding contact," *KMUTNB Int J Appl Sci Technol*, vol. 11, no. 1, pp. 63–72, Jan.–Mar. 2018.

the brake disc is converted into heat due to the friction between brake pad and brake disc. Heating and cooling of the brake discs can cause deformation, which effects the braking process. The high temperature generated at the interface of brake disc and brake pad during the braking process can cause brake fade and thermal cracks, which affects the braking performance. The frictional heat generated during braking causes thermoelastic distortion that modifies the contact pressure distribution [1].

Wear in brake discs occurs as a result of frictional contact between brake disc and brake pad and due to the relative motion of the pressed pad fixed against the rotating disc. Wear is defined as damage to a solid surface, which involves progressive loss of material, due to relative motion between the surfaces of contacting substances [2]. In fact, wear is a system's response, not a material property [3].

Wear in brake discs occurs because of different mechanisms that may include fatigue wear, corrosive wear, fretting wear, adhesive wear, abrasive wear and thermal wear. However, the predominant mechanisms are adhesive and abrasive wear. It depends upon different parameters, which can be divided into three main categories:

1. Operating parameters, including contact pressure, velocity, sliding distance, surface temperature and surface finish.

2. Material parameters, including material properties like toughness, melting point, thermal conductivity, ultimate tensile strength and electrochemical potential.

3. Environmental parameters, including humidity and heat radiation level.

Wear reduces the thickness of the brake disc and brake pad, which is a safety critical problem, because manufactures usually define an optimum thickness for better braking performance. Wear of disc brakes generates airborne particles, which are dangerous for the human health because it can lead to diseases like irritation of eyes and inflammation of the respiratory track, which can cause cancer. Therefore, the investigation of temperature and wear variations of brake discs and brake pads during braking conditions is important.

Two types of methods exist in the literature for calculating wear, namely micro-scale and macro-scale. The micro-scale approach is based on the failure criteria and the macro-scale approach is based on empirical wear equations. Different wear models exist in the related literature for investigating wear at the macro-scale level. Rhee [4] proposed a wear model, which is based on applied load, speed and time. Barwell [5] proposed a wear model based on experimental investigations and comprising three empirical equations. Archard [6] proposed a wear model for sliding wear taking the specific sliding, adhesion, sliding speed and contact pressure into account. This model is the most widely used to simulate wear in general sliding contacts.

Podra and Andersson [7] calculated sliding wear with the finite element method by using Archard's wear law. Molinari *et al*. [8] used Archard's wear law to calibrate and validate a finite element model of dry sliding wear in metals. Hegadekatte *et al*. [9] used Archard's wear law to develop a predictive modeling scheme for wear in tribometers. Benabdallah and Olender [10] used Archard's wear law for finite element simulations of the wear of polyoxymethylene. In the past (1980–2000), wear models were developed based on wear maps. The main aim of these models was to identify the main mechanism of material loss from the surfaces. A wear map for steel was developed by Lim and Ashby [11], for ceramic by Hsu and Shen [12] and for magnesium alloy by Chen and Alpas [13].

In the past, various researchers developed finite element models to investigate thermo-mechanical behavior of disc brakes. Koetniyom *et al*. [14] developed a material model for cast iron that is used for brake system analysis. They have considered repeated braking conditions and performed sequentially coupled thermo-mechanical finite element analysis of disc brakes. Dufrénoy and Weichert [15] developed a thermo-mechanical model to analyze the fracture mechanisms of disc brakes. Dufrénoy [16] proposed a macrostructural model of the thermo-mechanical behavior of disc brakes, which comprises of an uncoupled iterative algorathim. Zhao *et al*. [17] developed a coupled thermo-mechanical model in order to analyze the behavior of a composite multidisc clutch. Kao *et al*. [18] developed a 3D thermo-mechanical, finite element model to investigate hot judder in a disc brake. They concluded that buckling instability is a significant factor, which can cause hot spots and hot judder. Lamjahdy *et al*. [19] studied the decoupled thermo-mechanical simulation of macroscopic hot spots in railway disc brakes. Lamjahdy *et al*. [20] investigated the thermo-mechanical and wear behavior

of a disc brake. Moreover, they [21] proposed a coupled thermo-mechanical model in combination with a Hertz contact formulation to predict hot spotting in disc brakes. Markert [22] surveyed selected coupled multifield problems in computational mechanics and presented an appropriate classifications of coupled equation systems.

In the present research, a simulation methodology is introduced for investigating an uncoupled thermo-mechanical and wear behavior of engineering materials (here: aluminium on cast iron) in sliding contacts. The uncoupled thermo-mechanical analysis is based on frictional heat contact calculations, and the wear analysis is based on Archard's wear law. The developed numerical model is calibrated and validated with the experimental results.

2 Experimental Investigation

The experimental investigations were performed in our laboratory by using a pin-on-disc test bench. The complete design and development of the test bench is accomplished at the Institute of General Mechanics (IAM), RWTH Aachen University, Germany. The pin-on-disc test bench is a simple experimental setup, which is commonly used for investigating wear in general sliding contacts and for obtaining reproducable results. In the experiment, a pin is pressed against a rotating disc. The load is usually applied on the pressed pin and the disc is rotating at a pre-defined rotational speed. The load on the pin, the rotational velocity of the disc and the geometries of the pin and disc can be varied in order to analyze the problem of interest. The experimental investigations followed the procedure of test method G99 ASTM [23] with different materials (here: aluminium pin on cast iron disc) and with different input parameters, i.e. load on pin, braking time and rotational velocity of disc. The pin-on-disc test bench, as shown in Figure 1, is composed of lever arm, pin, mass, disc, fixed bearing and motor. The motor actuates the disc and the lever arm presses the pin against the rotating disc.

The real experimental setup, as shown in Figure 2(a), entails a stationary cylindrical pin fixed against the rotating disc. The desired load is enforced on the stationary pin via a lever arm. The material aluminium is used for the stationary cylindrical pin. A thermocouple, see Figure 2(b), measures the temperature inside the pin.

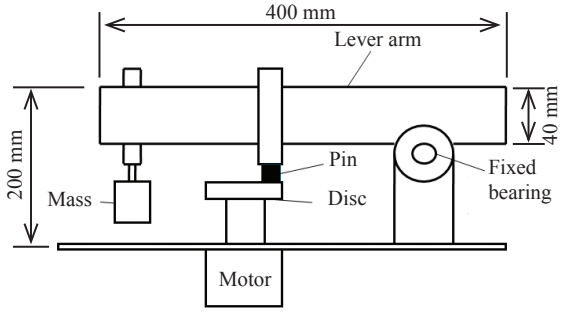

Figure 1: Schematic of a pin-on-disc test bench.

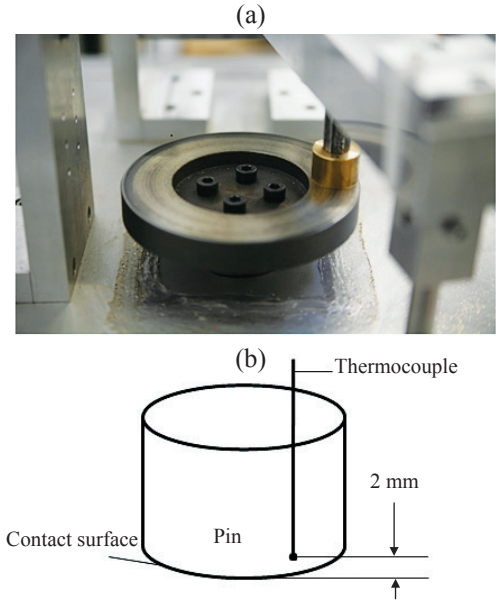

Figure 2: Experimental setup: (a) Pictorial view of pressed pin fixed against the rotating disc. The outer diameter of the pin is 28 mm and outer diameter of the disc is 140 mm. (b) Point of measurement of temperature inside the pin by using a thermocouple.

The point of measurement of the temperature is 2 mm above the contact surface.

2.1 *Experimental procedure*

The veracity of the experimental results relies on a proper contact between the disc and the pin. Therefore, to achieve proper contact surfaces at the interface of the disc and the pin, the experimental setup is run for half an hour before performing actual experiments. Mass are attached at the end of the lever arm and

the motor is aasigned with a rotational velocity. The thermocouple measures the temperature variations inside the pin. In current study, two experimental cases are being performed by varying input parameters i.e. load on the pin and rotational speed of the disc. The total mass loss is measured by weighing the initial mass of the pin (at the start of experiment) and the final mass of the pin (at the end of experiment). The net difference between the final mass and the initial mass is the total mass loss.

The input parameters for the experimental cases are given in Table 1.

Table 1: Experimental case with input parameters

Test Case	Rotational Velocity (rpm)	Load on Pin (N)	Braking Time(s)
1	300	110	30
2	600	150	30

2.2 *Experimental results*

The wear rate is calculated from experimental data and used in the numerical wear analysis. In particular, the wear rate is governed by the implementation of Archard's wear law [Equation (1)]:

$$k_d = \frac{v_{loss}}{sf}. \quad (1)$$

Herein, k_d is the wear rate ($m^2\ N^{-1}$), s is the sliding distance (m), f is the load on the pin (N) and v_{loss} is the volume of material loss (m^3) calculated from the Equation (2)

$$v_{loss} = \frac{m_{loss}}{\rho}, \quad (2)$$

where ρ is the density of the material (kg m^{-3}) and m_{loss} is the mass of the material (kg). The wear rate calculations are given in Appendix A. The results from the experimental investigations are given in Table 2.

Table 2: Experimental results

Test Case	Initial Mass (g)	Final Mass (g)	Mass Loss (g)	Volume Loss (m^3)	Wear Rate ($m^2\ N^{-1}$)
1	67.0	66.94	0.056	$2.07\ 10^{-8}$	$3.74\ 10^{-12}$
2	66.0	65.9	0.1	$3.70\ 10^{-8}$	$2.42\ 10^{-12}$

The mass loss for the test case 1 is determined to be 0.056 g and the wear rate (k_d) is calculated as $3.74\ 10^{-12}\ m^2\ N^{-1}$, which is used in the numerical wear analysis. Similarly, the mass loss for the test case 2 is determined to be 0.1 g and the wear rate is calculated as $2.42\ 10^{-12}\ m^2\ N^{-1}$, which is used in the numerical wear analysis. The initial temperature for the test case 1 is 18°C and the measured final temperature at the end of the braking process is observed as 65°C. Similarly, the initial temperature for the test case 2 is 18°C and the measured final temperature at the end of the braking process is observed as 97°C.

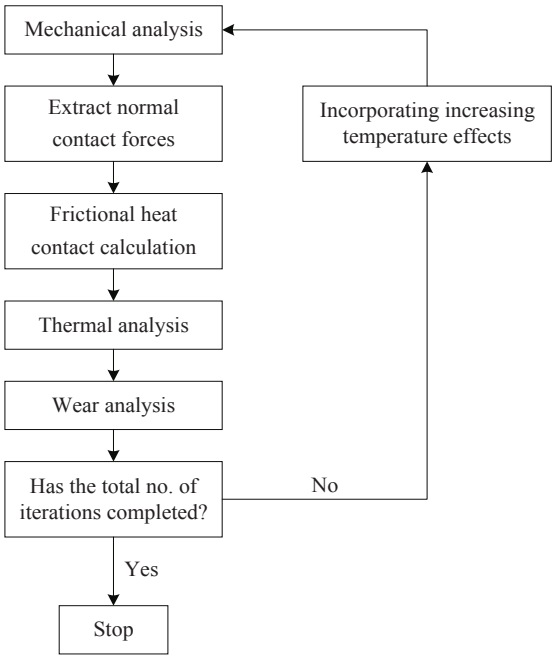

Figure 3: Simulation methodology flow chart.

3 Numerical Modeling

A simulation methodology has been developed in order to investigate uncoupled thermo-mechanical and wear simulations in general dry sliding contacts. The Abaqus scripting interface via the python programming language has been used to develop the simulation methodology. There are solution steps combined with additional calculation steps in the simulation workflow as shown in Figure 3. The overall simulation methodology is divided into three main steps:

1. Mechanical analysis,
2. Thermal analysis,
3. Wear analysis.

The first step is the mechanical analysis [Equation (3)], which involves the calculation of the normal contact forces at the interface of the disc and the pin.

$$\sigma(x,t) = C^4 [\varepsilon^e (x,t) - \alpha(T(x,t))\Delta T(x,t)I]. \quad (3)$$

The normal contact forces calculated from the Equation (3) are then used in the frictional heat contact calculation, which represents the total work done by the frictional force given by [Equation (4)]

$$q = f_N \mu v. \quad (4)$$

Herein, $\sigma(x,t)$ is the stress tensor (N m^{-2}), C^4 is the elasticity tensor (N m^{-2}), $\varepsilon^e (x,t)$ is the elastic strain tensor, $\alpha(T(x,t))I$ is the isotropic thermal expansion tensor (K^{-1}), q is the generated heat (J), f_N is the normal contact force (N), μ is the coefficient of friction and v is the sliding velocity (m s^{-1}).

The total heat generated calculated from the Equation (4) will be distributed among the contacting bodies, i.e. disc and pin [Equation (5)],

$$q_{Total} = q_{disc} + q_{pin} = (1-k_{pin})\, q + k_{pin}\, q, \quad (5)$$

where k_{pin} is the ratio of the heat partition representing the pin side.

The calculated frictional heat generated at the interface of the disc and the pin at each contacting node is subsequently used as a point heat flux boundary condition for the thermal analysis. The disc and the pin dissipate the heat produced at the boundary between the brake disc and the pin by convection and radiation. The model includes heat conduction in the brake disc and the pin through the transient heat transfer analysis given by [Equation (6)]

$$\nabla(-k\nabla T) + \rho\, c\, \Delta T = Q - \rho\, c\, u\, \nabla T. \quad (6)$$

Herein, Q is the heating power per unit volume (W/m^3), ρ is the density of material (kg/m^3), c is the specific heat capacity (J/kg K), k is the thermal conductivity (W/m K).

In a third step, the wear analysis is performed, which is based upon Archard's wear law. The nodal wear increments are calculated from

$$\Delta h_i = p_i\, k_d\, v\, \Delta t. \quad (7)$$

Herein, p_i is the nodal contact pressure (Pa) at the node i, which is calculated from the Equation (3), k_d is the wear rate (m^2 N^{-1}), v is the sliding velocity (m s^{-1}) and Δt is the time increment (s).

The nodal wear increment calculated from Equation (7) is then used to calculate the total volume loss [Equation (8)]:

$$v_{loss} = h_i\, a_i. \quad (8)$$

The total volume loss is then used to calculate the total mass loss via [Equation (9)]

$$m_{loss} = v_{loss}\, \rho, \quad (9)$$

where h_i is the nodal wear increment (m), a_i is the apparent contact area of the pin on the disc (m^2) and ρ is the density of the pin (kg m^{-3}).

The simulation methodology is assigned with the pre-defined value for the number of iterations. If the disc has completed its number of iterations, the simulation will be stopped. If not, further iteration has to continue by incorporating increased temperature due to the frictional heat effect at the contact interface in the mechanical analysis.

4 Finite Element Procedure

The Finite Element Method (FEM) provides a suitable method to generate a discrete algorithm to approximate the solution of the governing partial differential equations. FEM divides a larger problem into smaller parts, equations are created for each part which are then assembled together to provide a solution for the entire problem. The method uses discretization and numerical methods to solve partial differential equations for complex geometries which cannot be solved by analytical methods. For this research, the commercially available finite element solver Abaqus is selected. Abaqus/CAE is used to generate the geometric model, which comprises of two main parts, namely pin and disc. Both parts are modeled as solid, 3D deformable bodies. The length of the pin is 20 mm and the diameter is 28 mm. The outer diameter of the disc is 140 mm. Both parts are meshed with eight node linear brick elements (C3D8) for the mechanical analysis and with eight node linear heat transfer brick elements (DC3D8) for the thermal analysis. The disc consists of

3266 elements and the pin consists of 2739 elements. The model is assigned with an initial temperature of 18°C. Abaqus/Standard is used as solver in the current research. The pin is assigned with the material properties of aluminium and the disc is assigned with the properties of cast iron (GG-25). All material properties are given in Table 3.

Table 3: Material properties of finite element model

	Disc	Pin
Thermal expansion [1/K]	1.2 10^{-11}	2.3 10^{-5}
Thermal conductivity (W/m K)	50	170
Specific heat (J/kg K)	490	900
Young's modulus (N/m^2)	1.17 10^{11}	6.9 10^{10}
Density (kg/m^3)	7200	2700
Poisson's ratio	0.26	0.33

The pin is fixed against the disc by constraining its movement in x and y direction. The load is applied on the top surface of the pin and a rotational velocity is assinged to the disc. The load cases for the simulations are the same as used in the experiments. The boundary conditions prescribed as given in Table 1.

The boundary conditions and mesh of the finite element model are shown in Figure 4.

In order to assemble the pin with the disc, positional constraints are used. Surface to surface contact is assigned between the disc and the pin. In particular, frictional contact is used during the mechanical analysis and thermal conductance contact is used during the thermal analyis.

5 Results and Discussions

The temperature and wear variations of aluminium are studied. The experimental investigations are performed by using the pin-on-disc test bench and the numerical investigations are carried out by using the developed simulation methodology implemented in Abaqus. The results from both the experimental and numerical investigations are discussed, compared and validated in the following paragraphs.

5.1 *Normal contact pressure distribution pin*

The pressure distribution at the interface of the pin in contact with the disc for the test case 1 is shown in Figure 5 and for the test case 2 in Figure 6. Figures 5(a)

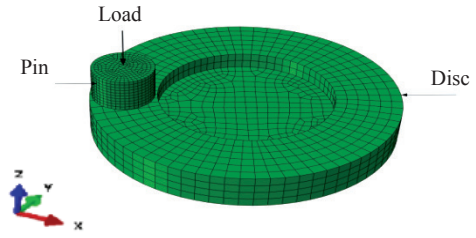

Figure 4: Mesh and boundary conditions of the finite element model.

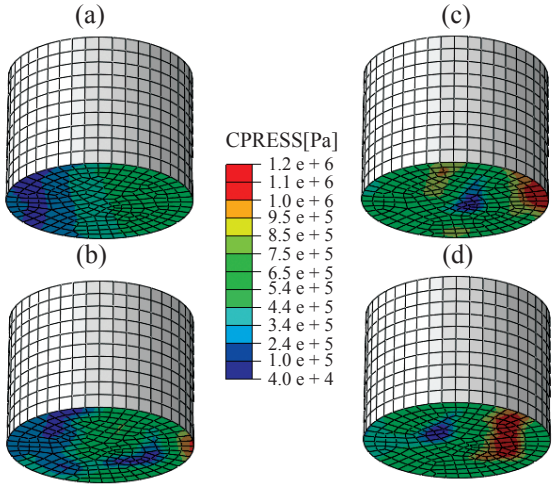

Figure 5: Contact pressure distribution on pin after (a) No. of rev. =10, (b) No. of rev. =50, (c) No. of rev. =100 and (d) No. of rev. =150.

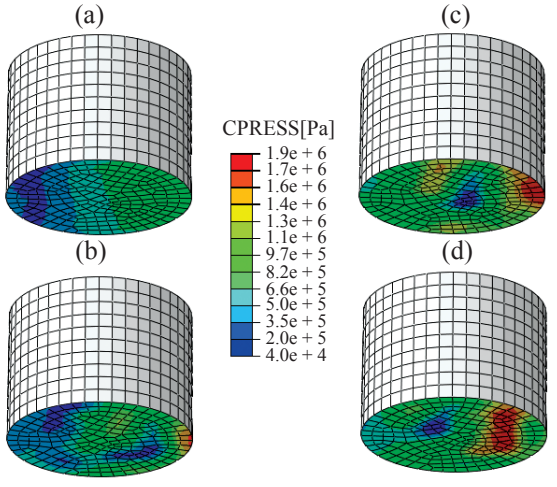

Figure 6: Contact pressure distribution on pin after (a) No. of rev. =10, (b) No. of rev. =100, (c) No. of rev. =200 and (d) No. of rev. =300

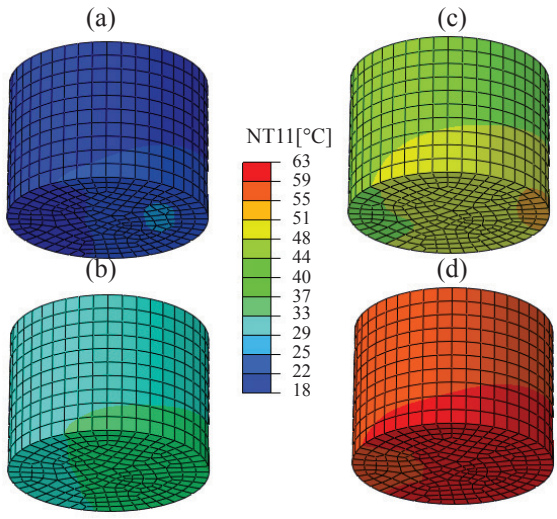

Figure 7: Temperature distribution of pin after (a) No. of rev. = 10, (b) No. of rev. = 50, (c) No. of rev. = 100 and (d) No of rev. = 150.

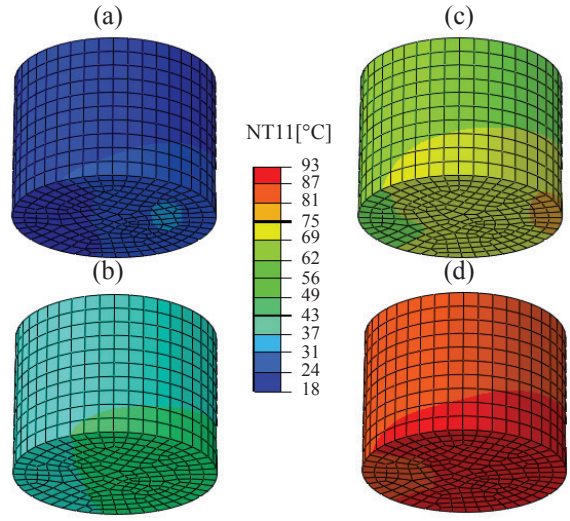

Figure 8: Temperature distribution of pin after (a) No. of rev. = 10, (b) No. of rev. = 100, (c) No. of rev. = 200 and (d) No of rev. = 300.

to (d) show the normal contact pressure distribution for the test case 1 on the pin after 10, 50, 100 and 150 revolutions, respectively.

Figures 6(a)–(d) show the normal contact pressure distribution for the test case 2 on the pin after 10, 100, 200 and 300 revolutions, respectively.

A maximum pressure of 1.2 10^6 Pa for the test case 1 and 1.9 10^6 for the test case 2, and a minimum pressure of 4.0 10^4 Pa for the test case 1 and 4.0 10^4 Pa for the test case 2 is observed.

The maximum pressure occurs towards the inner ring of the pin while the minimum pressure is observed at the outer ring of the pin. A previous study of contact pressure distribution [24] carried out for a pad to rotor interface showed the same effects for normal contact pressure distribution, i.e. the concentration of normal contact pressure is increasing with the values of the number of revolutions.

5.2 *Temperature distribution pin*

The temperature distribution of the pin for the test case 1 is shown in Figure 7 and for the test case 2 in Figure 8. Figures 7(a)–(d) show the temperature distribution of the pin after 10, 50, 100, and 150 revolutions, respectively.

Figures 8(a)–(d) show the temperature distribution of the pin after 10, 100, 200, and 300 revolutions, respectively.

The initial temperature is 18°C for the test case 1, while the observed maximum temperature at the end of the braking process for the test case1 is 63°C. Similarly, the initial temperature for the test case 2 is 18°C, while the observed maximum temperature at the end of the braking process for the test case 2 is 93°C. The maximum temperature is observed towards the inner ring of the pin and the minimum temperature is observed towards the outer ring of the pin. Heat is conducting from the inner ring towards the outer ring and from the contact surface towards the upper region. The temperature distribution depicts that the simulation is stable and that the temperature is increasing with the number of revolutions. Our previous study of the temperature distribution [20] carried out for a pin in contact with a disc showed the same effects. The values of temperatures are increasing with the number of revolutions.

5.3 *Result validation*

The experimental and the numerical investigation results are validated and compared as shown in Figure 9. On the horizontal axis is the braking time and on the vertical axis is the temperature distribution.

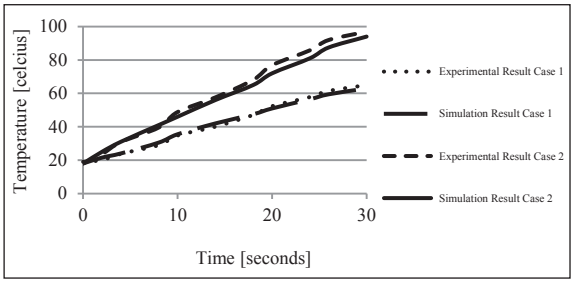

Figure 9: Comparison between experimental and numerical results.

During the experimental investigation, temperature is measured inside the pin 2 mm above the contact surface, see Figure 2(b). In the simulation, the values of temperature are measured at the node in the FE model that is in the position of the thermocouple. For the test case 1, the numerical investigation shows a maximum temperature of 63°C and the experimental investigation shows a maximum temperature of 65°C. A difference of 2°C is observed. Similarly, for the test case 2 the numerical investigation shows a maximum temperature of 93°C and the experimental investigation shows a maximum temperature of 97°C. A difference of 4°C is observed. The experimental results are in close agreement with the numerical results. For the test case 1, total worn mass calculated during the numerical investigation is 0.0054 g and the measured value during the experimental investigation is 0.0056 g. That is 3.5% error between the results of the experimental and the numerical investigation. For the test case 2, total worn mass calculated during the numerical investigation is 0.12 g and the measured value during the experimental investigation is 0.10 g. That is 16.6% error between the results of the experimental and the numerical investigation. Possible sources of error in the current study includes instrumental errors, human errors, vibrational effects and environmental effects. The result shows that the developed numerical model is accurate and can be used to investigate mechanical and thermal stresses, deformation, temperature and wear variations of different materials in general dry sliding contacts.

6 Conclusions

In this research paper, an experimental and numerical study is performed to investigate the temperature and wear variations of aluminium in dry sliding contact. The numerical investigation is done by means of a developed simulation methodology implemented in the commercially available finite element solver Abaqus. The experimental investigations are performed by using a pin-on-disc test bench. Comparison between the experimental and the numerical investigation reveals the good accordance of the simulation model and the experiment. Therefore, it is confirmed that the developed numerical model is accurate and can be used to calculate temperature, wear depth and mass of material loss at the interface of brake disc and brake pad during braking conditions. The results from this research can be used to predict the service life of the brake disc and the brake pad and to solve comfort related problems of passengers.

A linear elastic material model has been used for the numerical investigation. Possible areas of future work includes:

1. Usage of temperature-dependent and nonlinear material properties for numerical investigation.
2. Usage of profilometer in experiments to measure the wear depth at regular intervals.
3. Usage of adaptive meshing to account for the damage accumulation caused by the surface wear.
4. Implementation of non-linearity in Archard's wear law.

Acknowledgments

This research was funded by the Institute of General Mechanics (IAM), RWTH Aachen University, Germany. The authors would like to convey sincere thanks to all the employees and colleagues working at the Institute of General Mechanics for their support and guidance.

References

[1] S. Du and J. Fash, "Finite element analysis of frictionally-excited thermo-elastic instability in 3D annular disk," *International Journal of Vehicle Design*, vol. 23, no. 3, pp. 203–217, 2000.

[2] *Standard terminology relating to wear and erosion, American Society for Testing and Materials*, Standard G40, 2005.

[3] R. G. Bayer, *Mechanical Wear Prediction and Prevention*. New York: M. Dekker, 1994, pp. 280.

[4] S. K. Rhee, L. Halberstadt, and J. A. Mansfield,

Wear of Materials. New York: ASME, 1977, pp. 560–568.

[5] F. T. Barwell, "Wear of machine elements," in *Fundamentals of Tribology*, Cambridge, Massachusetts: The Mit Press, pp. 401–441, 1978.

[6] *Wear control handbook*, The American Society of Mechanical Engineers, New York, US, 1980.

[7] P. Podra and S. Andersson, "Simulating sliding wear with finite element method," *Tribology International*, vol. 32, pp. 71–81, 1999.

[8] J. F. Molinari, M. Ortiz, R. Radovitzky, and E. A. Repetto, "Finite-element modeling of dry sliding wear in metals," *Engineering Computations*, vol. 18, no. 3/4, pp. 592–609, 2001.

[9] V. Hegadekatte, S. Kurzenhauser, N. Huber, and O. Kraft, "A predictive modeling scheme for wear in tribometers," *Tribology International*, vol. 41, pp. 1020–1031, 2008.

[10] H. Benabdallah and D. Olender, "Finite element simulation of the wear of polyoxymethylene in pin-on-disc configuration," *WEAR*, vol. 261, pp. 1213–1224, 2006.

[11] S. C. Lim and M. F. Ashby, "Wear-Mechanism Maps," *Acta Metall*, vol. 35, no. 1, pp. 1–24, 1987.

[12] S. M. Hsu, M. C. Shen, and A. W. Ru, "Wear prediction for metals," *Tribology International*, vol. 30, pp. 377–383, 1997.

[13] H. Chen and A. T. Alpas, "Sliding wear map for the magnesium alloy Mg-9al-0.9 Zn (Az91)," *WEAR*, vol. 246, pp.106–116, 2000.

[14] S. Koetniyom, P. Brooks, and D. Barton, "The development of a material model for cast iron that can be used for brake system analysis," *SAGE Journal*, vol. 216, no. 5, pp. 349–362, 2002.

[15] P. Dufrénoy and D. Weichert, "A thermomechanical model for the analysis of disc brake fracture mechanisms," *Journal of Thermal Stresses*, vol. 26, no. 8, pp. 815–828, 2003.

[16] P. Dufrénoy, "Two-/three-dimensional hybrid model of the thermomechanical behaviour of disc brakes," *SAGE Journal*, vol. 218, no. 1, pp. 17–30, 2004.

[17] S. Zhao, G. E. Hilmas, and L. R. Dharani, "Behavior of a composite multidisk clutch subjected to mechanical and frictionally excited thermal load," *WEAR*, vol. 264, pp.1059–1068, 2008.

[18] T. Kao, J. Richmond, and A. Douarre, "Brake disc hot spotting and thermal judder: An experimental and finite element study," *International Journal of Vehicle Design*, vol. 23, no. 3, pp. 276–296, 2000.

[19] A. Lamjahdy, J. F. Brunel, B. Lamure, P. Dufrenoy, D. Weichert, and B. Markert, "The cyclic thermomechanical coupled problem of thermal gradients in friction railway disc brakes," *PAMM*, vol. 14, no. 1, pp. 461–462, 2014.

[20] A. Lamjahdy, J. Ali, and B. Markert, "Simulation of the temperature and wear behavior of disc brake," *PAMM*, vol. 16, no. 1, pp. 217–218, 2016.

[21] A. Lamjahdy, N. Moussa, M. Hirtz, P. Dufrenoy, D. Weichert, H. Murrenhoff, and B. Markert, "Simulation of thermal gradients on hot bands of disc brakes," presented at Euro Brake 2015, Dresden, Germany, May 4–6, 2015.

[22] B. Markert, "A survey of selected coupled multifield problems in computational mechanics," *Journal of Coupled Systems and Multiscale Dynamics*, vol. 1, pp. 22–48, 2013.

[23] Standard Test Method for Wear Testing with a Pin-on-Disk Apparatus, *American Society for Testing and Materials*, Standard G99, 2005.

[24] A. Söderberg and S. Andersson "Simulation of wear and contact pressure distribution at the pad-to-rotor interface in a disc brake using general purpose finite element analysis software," *WEAR*, vol. 267, pp. 2243–2251, 2009.

Appendix A

Wear Rate Calculations

The wear rate is governed by the implementation of Archard's wear law:

$$k_d = \frac{v_{loss}}{s\,f}\,. \qquad (1)$$

Herein, k_d is the wear rate ($m^2\ N^{-1}$), s is the sliding distance (m), f is the load on the pin (N) and v_{loss} is the volume of material loss (m^3).

The sliding distance s (m) is calculated from

$$s = 2\,\pi\,r\,N, \qquad (2)$$

where r is the distance from the center of brake disc to the center of the pin and N is the no. of rotations of brake disc.

The volume of material loss is calculated from

$$v_{loss} = \frac{m_{loss}}{\rho}, \qquad (3)$$

where ρ is the density of the material (kg m^{-3}), m_{loss} is the mass of material loss (kg). The total mass loss is measured by weighing the initial mass of the pin (at the start of the experiment) and the final mass of the pin (at the end of the experiment). The net difference between the final mass and the initial mass is the total mass loss.

Wear Rate Calculations for the Test Case 1

Input Values:

m_{loss} (kg) = 0.000056
ρ (kg m^{-3}) = 2700
N = 150
f (N) = 110
r (m) = 0.054

Output Values:

$$v_{loss} = \frac{m_{loss}}{\rho} = \frac{0.000056}{2700} = 2.07\ 10^{-8}\ m^3$$

$$S = 2\,\pi\,r\,N = 50.96\ m$$

$$k_d = \frac{v_{loss}}{s\,f} = \frac{2.07\ 10^{-8}}{50.96\ 110} = 3.74\ 10^{-12}\ m^2\ N^{-1}$$

Wear Rate Calculations for Test Case. 2

Input Values:

m_{loss} (kg) = 0.00001
ρ (kgm^{-3}) = 2700
N = 300
f (N) = 150
r (m) = 0.054

Output Values:

$$v_{loss} = \frac{m_{loss}}{\rho} = \frac{0.00001}{2700} = 3.703\ 10^{-8}\ m^3$$

$$S = 2\,\pi\,r\,N = 101.92\ m$$

$$k_d = \frac{v_{loss}}{s\,f} = \frac{3.703\ 10^{-8}}{101.92\ 150} = 2.422\ 10^{-12}\ m^2\ N^{-1}$$